PAPER

High pressure inertial focusing for separating and concentrating bacteria at high throughput

IOP Publishing Journal of Micromechanics and Microengineering
J. Micromech. Microeng. **27** (2017) 084001 (6pp) https://doi.org/10.1088/1361-6439/aa6b14

High pressure inertial focusing for separating and concentrating bacteria at high throughput

J Cruz[1], S Hooshmand Zadeh[1], T Graells[1,2,3], M Andersson[1], J Malmström[1], Z G Wu[1,4] and K Hjort[1]

[1] Engineering Sciences, Uppsala University, Ångström Laboratoriet, Uppsala, Sweden
[2] Department of Medical Biochemistry and Microbiology, Uppsala University, Uppsala, Sweden
[3] Departament de Genètica i Microbiologia, Universitat Autònoma de Barcelona, Barcelona, Spain
[4] State Key Laboratory of Digital Manufacturing Equipment and Technology, Huazhong University of Science and Technology, Wuhan, People's Republic of China

E-mail: javier.cruz@angstrom.uu.se and klas.hjort@angstrom.uu.se

Received 31 January 2017, revised 15 March 2017
Accepted for publication 4 April 2017
Published 27 June 2017

Abstract

Inertial focusing is a promising microfluidic technology for concentration and separation of particles by size. However, there is a strong correlation of increased pressure with decreased particle size. Theory and experimental results for larger particles were used to scale down the phenomenon and find the conditions that focus 1 μm particles. High pressure experiments in robust glass chips were used to demonstrate the alignment. We show how the technique works for 1 μm spherical polystyrene particles and for *Escherichia coli*, not being harmful for the bacteria at 50 μl min^{-1}. The potential to focus bacteria, simplicity of use and high throughput make this technology interesting for healthcare applications, where concentration and purification of a sample may be required as an initial step.

Keywords: bacteria separation, particle separation, inertial focusing, high pressure, glass chips, PDMS, microfluidic channel

(Some figures may appear in colour only in the online journal)

1. Introduction

Microfluidic systems offer features that differ from macro scale fluidics. By taking advantage of these features new applications have been developed intensely throughout the last decades, e.g. microfluidic chips that focus, concentrate, separate, transfer and mix particles and fluids have been presented. However, regarding particle separation not much progress has been made as we approach the sub-micro realm.

Inertial focusing is a phenomenon where suspended particles are separated by size in a microchannel. They migrate across streamlines and focus at well-defined, size dependent equilibrium points of the cross section. There is a necessity of large velocity gradients in the fluid to influence particles while a laminar flow is maintained. Such configuration is only possible at micro scale, which is the reason for the lack of observation of similar behavior at larger scale. Briefly, inertial focusing in straight channels is caused by the balance of two forces [1], see figure 1(A).

A shear lift force directed towards the walls of a channel due to the parabolic shape of the velocity profile ($F_{L\ SHEAR\ GRADIENT}$) and a wall lift force directed towards the center due to interactions of the streamlines with the wall ($F_{L\ WALL\ EFFECT}$, which decays with the distance to the boundaries). The net lift force (F_L) was theoretically predicted by Asmolov [2]:

$$F_L = \frac{4\rho C_{\mathrm{L}} U_{\mathrm{f}}^2 a_{\mathrm{p}}^4}{D_{\mathrm{h}}^2} \tag{1}$$

where ρ is the fluid density, C_{L} is the lift coefficient which is a function of the particle position across the channel cross-section and the channel Reynolds number, U_{f} is the average

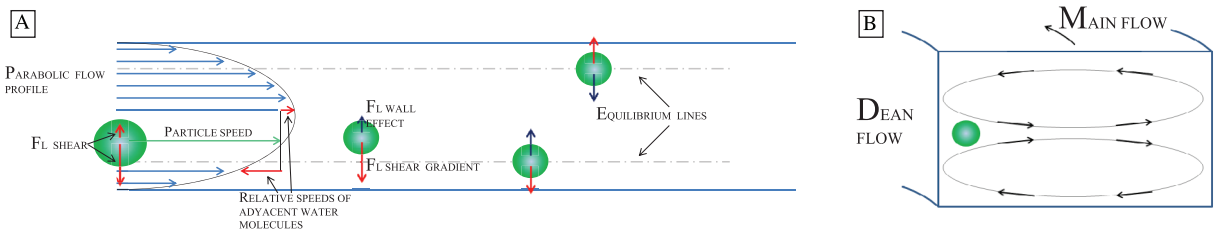

Figure 1. (A) Main forces in a straight microchannel. (B) Secondary flow due to centrifugal forces.

flow velocity, a_p is the particle diameter and $D_h = \frac{4(hw)}{h+w}$ the hydraulic diameter of the channel, with h its height and w its width.

As particles move across the streamlines pushed by the lift forces, a drag force (F_D) of the same magnitude but opposite direction arises and sets the maximum migration speed (U_L):

$$F_D = 3\pi\mu a_p U_L \tag{2}$$

where μ is the dynamic viscosity of the fluid. On the one hand, the net lift force needs to be strong enough to make the particles migrate through the channel in a reasonable time. On the other hand, the drag force plays an important role in the focus by limiting the maximum transversal speed of the particles. It sets the migration speed and thus the focus length and it also makes it possible for the particles to remain at the equilibrium positions; i.e. if the migration speed is too fast the particles will escape the equilibrium points and keep traveling.

The addition of curvature to the channel induces an uneven centrifugal force (since such force is proportional to the square of the velocity and the velocity profile is a parabola) and enables the development of a secondary flow called Dean flow, which redistributes the velocity profile, enhancing the lateral motion of particles and thus reducing the focus length. Only one position remains stable and the enhancement of the lateral migration makes the particles reach the point within a shorter time than in straight systems [3], figure 1(B).

In this paper we provide a theoretical approach for the design of the channels and discuss its limitations. We also show experimental demonstrations on high pressure, high throughput inertial focusing for 1 μm particles and *E. coli*.

2. Analysis of the scaling laws to succeed in the alignment

The cross section and the flow rate need to be tailored to reach equilibrium of forces and to achieve focus at reasonable lengths. We used the presented equations as a guideline to find a scaling law that allows the transformation of a working system to target smaller particles. The main aim is to find what conditions make it possible for a targeted particle size to reach the equilibrium positions and remain stable in them. We considered a straight system in the transformations; the radius of curvature will induce a secondary flow that will enhance the transversal migration and define the focus distance but it will not be critical to define equilibrium positions [4].

Let us start the analysis from a channel that can focus a certain size of particles. At some point of the cross section there is a balance between $F_{L\ SHEAR\ GRADIENT}$ and $F_{L\ WALL\ EFFECT}$. Also, F_D is such that it allows a reasonable migration speed and particles that reach the equilibrium positions stay stable. We want to preserve these characteristics and a solution to do so is to keep the magnitude of the forces constant. Alas, as we scale down the size of the particle we have to compensate by scaling up the fluid velocity and scaling down the hydraulic diameter to the same degree. If we also keep a constant aspect ratio, the flow rate should be decreased linearly.

The limitation is that as particles decrease in size, higher velocities and smaller channels are needed, which turns into a large drop of pressure. At the same time, such tailored conditions are valid for the target size but not for a wide span around it; much larger particles will not fit in the channel and much smaller ones will not feel enough lift force.

Following the formula recommended by Fuerstman *et al* (equation (3)) for the pressure drop in rectangular cross section channels [5], fulfilling the conditions mentioned above will mean a growth of the pressure drop to the power of three with a linear shrinkage of the targeted particle size (if the same length is used).

$$\Delta P \approx \frac{Q\ 12\mu L}{h^3 w\left[1 - 0.630\frac{h}{w}\right]} \tag{3}$$

where Q is the flow rate and L the length of the channel.

However, as we decrease the width of the channel particles need to migrate less transversal distance, which will shorten the focus length (L_f):

$$L_f = \frac{U_f}{U_L}\, w. \tag{4}$$

The lateral migration velocity can be known by comparing F_L and F_D:

$$U_L = \frac{4\rho C_L U_f^2 (a_p)^3}{3\pi\mu D_h^2} \tag{5}$$

The average migration speed can be estimated using an average value of $C_L \sim 0.5$ [2, 6]. Then:

$$L_f = \frac{3\pi\mu D_h^2}{2\rho U_f (a_p)^3}\, w. \tag{6}$$

Since we are scaling down the particle size and the hydraulic diameter and scaling up the fluid speed, the required focus length will scale linearly with the size of the particle, allowing for shorter channels and thus reducing some pressure drop.

Table 1. Scaling factors to achieve focus of particles. A design that works for certain particle size can be scaled to target another particle size with the rules in the table.

Scaling relations	Particle size	Height	Width	Flow rate	Focus length	Average speed	ΔP
Scale factor	X	X	X	X	X	X^{-1}	X^{-2}

The pressure will then scale up quadratically. The scaling factors to maintain the magnitude of the forces and achieve focus are summarized in table 1.

3. Experimental details

Microfluidic chips that tolerate a few bars of pressure were fabricated with polydimethylsiloxane (PDMS, RT601, Wacker Chemie) and then bonded to a glass slide. PDMS was poured onto a SU-8 mold that was fabricated by UV lithography on a silicon wafer. It was cured for 1 h at 70 °C, peeled off the mold and inlets/outlets were pierced with a biopsy punch. To form the bond, the PDMS and glass surfaces were activated by plasma exposure with a corona discharger for 30 s prior to coming in contact. A hydrogen bond was formed, which became covalent after the samples were put into the oven at 70 °C for 30 min.

Microfluidic glass chips tolerant of pressures up to 200 bar were fabricated and assembled as described in [7]. Briefly, a borosilicate glass wafer was wet etched in concentrated HF using molybdenum as a mask. Inlets and flow channels were etched in two separate steps. The wafer was bonded to another borosilicate wafer and thermally treated at 625 °C. After dicing, silica capillaries were glued to the chip inlets to provide a fluid connection.

The design of the spiral included 6 mm of the channel with the predicted dimensions to focus 1 μm particles—10 × 24 μm ($h \times w$)—and 6 mm of a second, wider spiral—10 × 60 μm ($h \times w$)—only meant to connect such channel to the outlet, which was in the interface of the bonded wafers and was not accessible from the center. It was made wider to avoid pressure drop to some extent.

Fluorescent polystyrene particles (Thermoscientific Fluoro-Max) with diameters of 10, 3 and 1 μm were suspended in deionized water at a concentration of 10^5, 10^6 and 10^7 particles ml^{-1} respectively.

E. coli (rod shaped bacterium, 0.5–1 μm in diameter by 2–4 μm in length) carrying Yellow Fluorescent Protein (DA45134 strain *E. coli* MG1655 Δ(IS150)::CP25-yetiYFP) were suspended in sterile deionized water at a concentration of 10^8 cells ml^{-1}. Samples of the suspension were taken before and after passing through the chip at 50 and 100 μl min^{-1}. The concentrations were determined by optical density at a wavelength of 600 nm and by counting the colony forming units in cultures in LB agar plates (at 37 °C, aerobic conditions, 24 h). The viability was evaluated with the results from the culture.

A precision syringe pump (Harvard Apparatus, PHD 2000 infusion) was used to control the flow through the channels in the low pressure experiments (<10 bar) and a high pressure HPLC pump (Waters, model 515) in the high pressure experiments (<200 bar).

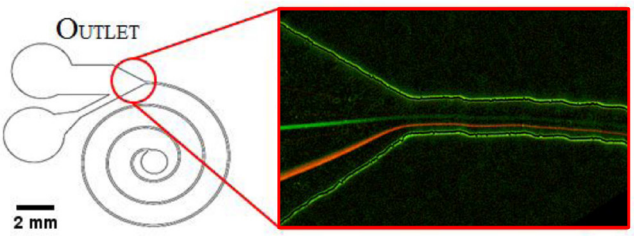

Figure 2. Equilibrium position for 10 μm (green) and 3 μm (red) particles in a curved microchannel—30 × 100 μm ($h \times w$)—at 200 μl min^{-1}.

Only pressure is needed to perform the separation by inertial focusing.

The experiments were carried out under a fluorescence inverted microscope.

4. Results

For the low-pressure control, we fabricated chips on PDMS that could focus 10 and 3 μm particles. We used the acquired data and the scaling laws described above to calculate the requirements for new channels that could work for 1 μm particles. The channels were then fabricated in glass chips and tested with 1 and 3 μm particles and *E. coli*.

4.1. Low-pressure PDMS chips

The phenomenon was first studied in straight microchannels with 10 μm particles. Adding curvature to the channels led to a single equilibrium position. Changing the height of the channel, 3 μm particles were focused close to the inner wall while those of 10 μm were displaced to the center, figure 2.

No focus was observed for 1 μm particles. A channel with predicted suitable dimensions for such particle size was tested—10 × 30 μm ($h \times w$)—but the high pressure led to leakage of the system.

4.2. High-pressure glass chips

The glass chips could tolerate up to 200 bar before cracking and were suitable to create the predicted conditions to focus 1 μm particles. The experimental results agree with the predictions, 1 and 3 μm particles and *E. coli* were aligned in a spiral with 1 mm as outer radius, figure 3.

A spiral whose radius was four times bigger also showed alignment of the particles although it took a longer distance.

4.3. E. coli viability

Both evaluation methods agree and showed similar concentrations of *E. coli* in the control and after the chip at a flow rate of 50 μl min^{-1}, which was driven at 70 bar of pressure. At 100 μl min^{-1}, which needed 150 bar, the number of

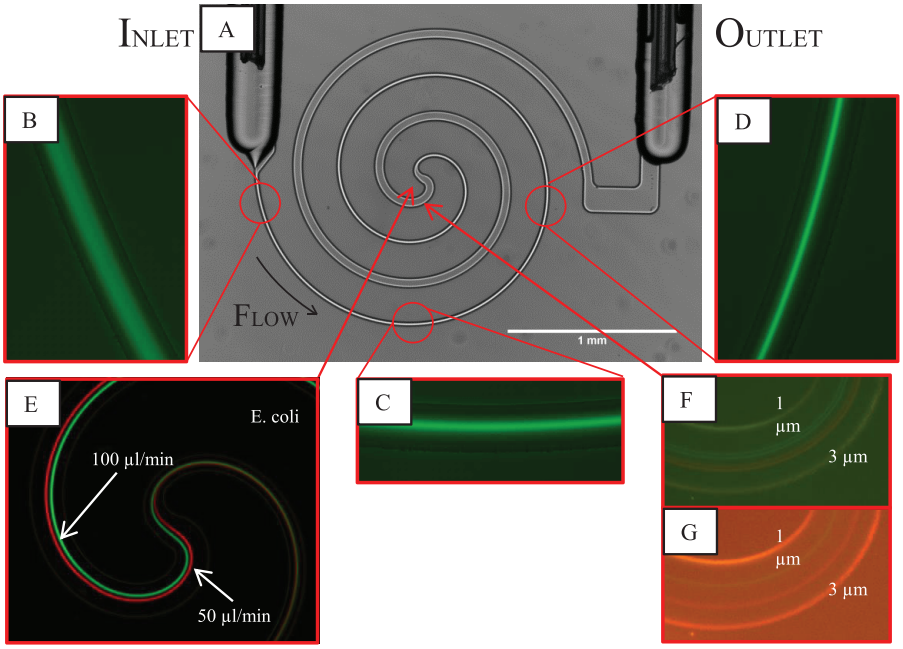

Figure 3. (A) Channels in a glass chip—10 × 24 μm in the narrow part and 10 × 60 μm in the wide part ($h \times w$). (B) Position of *E. coli* in the microchannel at 100 μl min^{-1} at the inlet (C) after 1/4 loop (D) after 1/2 loop. (E) Equilibrium position for *E. coli* at 50 and 100 μl min^{-1}. (F) Separation of 1 and 3 μm polystyrene particles at 100 μl min^{-1} and (G) at 200 μl min^{-1}.

bacteria decreased one order of magnitude, see table 3. The pressures were higher than those in the previous experiments with particles due to partial clogging of the inlet.

5. Discussion

Following the work of the group of di Carlo [1], the dimensions of the channel should be such that the smallest cross section of the particle should not be less than one tenth of the channel height (h) and the width (w) should also be matched to the height in a relation $h < w < 6h$. This statement agrees with our obtained results, where in a 30 × 100 μm channel the smallest particles we could focus were those of 3 μm since 1 μm particles did not meet the condition.

In the spiral with outer radius of 1 mm, the alignment of 3 μm particles was clear after ~1.5 mm (1/4 of loop) at 100 μl min^{-1}, of 1 μm particles after ~3.8 mm (3/4 of loop) and of *E. coli* after ~2.7 mm (1/2 loop), figures 3(B)–(D). *E. coli* behaved like a spherical particle of a diameter in between 1 and 3 μm, which is in accordance with previous studies, concluding that rod shaped particles behave as spherical particles with a diameter equivalent to their largest dimension [1]. Considering these focus lengths, most of the channel only contributes to an unnecessary pressure drop. The design can be optimized to less than one loop. This would allow alignment of 1 μm particles at more than double flow rate using the same pressure. More importantly, less than one loop short channels ease integration, since out-of-plane interconnects are not necessary.

Increasing the flow rate made the alignment faster and also shifted the equilibrium positions towards the outer wall for *E. coli*, figures 3(E) and 4. The behavior was similar for 1 μm particles while 3 μm particles moved closer to the inner wall (figures 3(F) and (G)—in these pictures the walls are shifted since the particles just passed the center of the spiral).

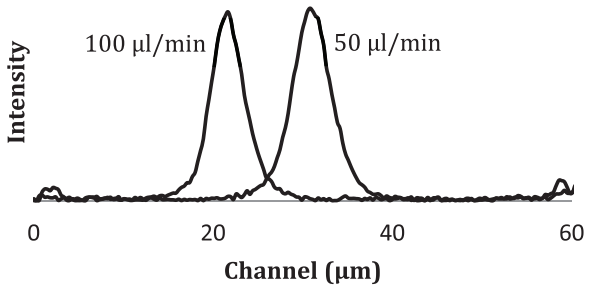

Figure 4. Position of *E. coli* in a transversal cut of the microchannel at 50 and 100 μl min^{-1}. The analysis was done in figure 3(E). In the X axis, 0 represents the inner wall and 60 the outer wall of the wide part of the channel.

Figures 3(F) and (G) show separation of 1 and 3 μm particles at different flow rates, having a larger separation at 200 than at 100 μl min^{-1}. The equilibrium lines split in two for each size at 100 μl min^{-1} (figure 3(F)) and merge or overlap at 200 μl min^{-1} (figure 3(G)). This is likely due to the shape of the cross section of the channel, which is not rectangular but with rounded lower corners, leading to two asymmetric Dean vortexes. This results suggest that not one but two equilibrium positions are available for each size in curved microchannels, being overlapped if the secondary flow is symmetrical and mismatched in our particular case (isotropically wet etched channels), figure 5.

In the PDMS chips, the smallest particles were aligned closer to the inner wall while the biggest were in the middle,

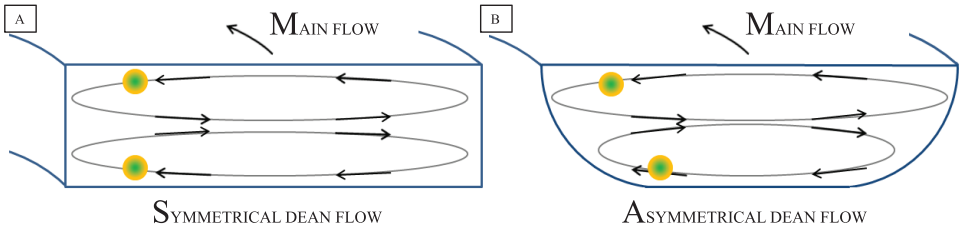

Figure 5. Difference of equilibrium positions in (A) symmetric and (B) asymmetric (wet etched) cross section channels.

Table 2. Application of the scaling laws. Microchannels that can focus 3 μm particles are scaled down to focus 1 μm particles. Predicted data is compared to experimental data for 1 μm particles.

	Particle size (μm)	Height (μm)	Width (μm)	Flow rate (μl min^{-1})	Focus length (mm)	Average speed (m s^{-1})	ΔP (bar)
Experimental	3	30	100	200	20	1.1	3.6
Scale factor	1/3	1/3	1/3	1/3	1/3	3	9
Predicted	1	10	30	70	7	3.3	32
Predicted	1	10	24	100	4.6	5.9	38
Experimental	1	10	24	100	3.8	5.9	44[a]
Predicted	0.44	4.4	10	44	2.0	16.7	200

[a]The pressure drop was 100 bar and was measured throughout the whole system, which had a total length of 12 mm. Using the narrow part as reference, the equivalent length is 8.4 mm. Thus, we estimated the pressure drop in 3.8 mm as 44 bar.

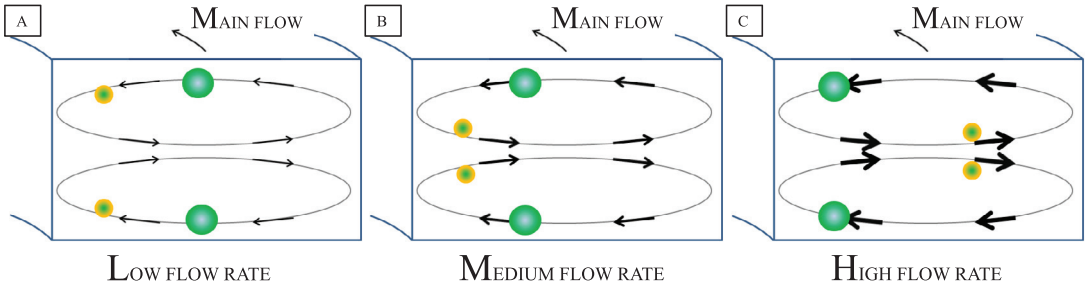

Figure 6. Equilibrium positions for different sizes as the fluid speed increases. (A) Case of our PDMS chips; low fluid speed. (B) Intermediate fluid speed. (C) Case of our glass chips; high fluid speed.

Table 3. Concentration and viability of *E. coli* before and after inertial focusing by optical density and by culture in agar.

	Cells ml^{-1} ($\times 10^7$)	
Sample	By OD	By culture
Control	20	34
50 μl min^{-1}—70 bar	32	54
100 μl min^{-1}—150 bar	3	2

figure 2. On the other hand, in the glass chips it was in reverse, the biggest particles were closer to the inner wall. An increase in the flow rate would push them even closer while the smallest were pushed further away (figures 3(E)–(G)). These facts together with the two equilibrium lines seen at low flow rates suggest the following equilibrium positions depending on the flow rate for a given curvature, see figure 6.

As shown in table 3, the concentration and viability of the samples of *E. coli* after being focused at 50 μl min^{-1} (70 bar) did not differ from the control, which makes the technique suitable for bacterial separation and concentration. However, their number was decreased by one order of magnitude at 100 μl min^{-1} (150 bar). The cause of death is likely to be the rapid, large pressure drop. To note, a flow rate of 50 μl min^{-1} with a cell concentration of 10^8 cells ml^{-1} still makes a throughput in the order of 100 000 cells s^{-1}. The pressure needed to keep a flow rate increased with time due to clogging of the inlet by aggregates or dirt. To solve this and minimize the pressure through the chip a filter should be added at the inlet.

The principal limitation of inertial focusing comes much before the limits of continuum and even before the electrical forces start to dominate, i.e. the realm of nanofluidics. Following the scaling laws stated in the paper, smaller particles require smaller cross sections and higher velocities, which lead to much higher pressures. If it takes 38 bar to focus 1 um particles, focus of 0.1 um particles would take 100 times higher pressure; i.e. 3800 bar. Thus, we consider pressure as the limitation of this technology.

For our chips, it should be possible to reach particles sizes down to 0.44 μm, table 2. However, other work has shown chips surviving 600 bar [8], which would enable particle focusing down to 0.25 μm, making the technology suitable

for nanoparticles or virus (if no harm is induced to them in the process).

As previously often shown [4], the final part of the channel can be widened and split into several outlets, achieving separation, purification and concentration of particles at high throughput.

6. Conclusion

Inertial focusing in microchannels offer a solution for separating, purifying and concentrating bacteria at high viability at high throughput ($Q = 50\ \mu\text{l min}^{-1}$) even if its cross section is in the sub-micron scale like the *E. coli*. The technique has the potential to focus even smaller organisms whose dimensions are in the sub-micron scale like *Legionella sp*, nanoparticles or viruses.

Key in scaling down the design is to keep the conditions that allow particles to migrate, reach the equilibrium points and remain in them in a stable way. This can be done by tailoring the dimensions of the cross section and the flow rate. Then the focus length can be optimized with the curvature.

Isotropically etched channels offered a new perspective that may help for further understanding of the phenomenon thanks to the asymmetrical secondary flow, where there is a visual mismatch of the two equilibrium positions for a single particle size.

The ability to focus sub-micron bacteria, simplicity of use and high throughput make this technology interesting for healthcare, where concentration and purification of a sample may be required as an initial step. Optimization of the chip can still be made, especially regarding the length, which will enable higher flow rates or smaller cross sections for the same pressure. Also, sub-one-loop curved channels can perform the separation and ease integration with other microfluidic steps on a chip.

Acknowledgments

We thank Lena Klintberg for all the support in the laboratory throughout the fabrication and evaluation processes, Erik Gullberg for constructing and providing the DA45134 strain *E. coli* MG1655 Δ(IS150)::CP25-yetiYFP and also Adrian Falk, Anton Rundberg and Johan Stjärnesund for their collaboration. The project has received funding from the European Union's Horizon 2020 research and innovation program under grant agreement no. 644669.

References

[1] Amini H, Lee W H and Di Carlo D 2014 Inertial microfluidic physics *Lab Chip* **14** 2739
[2] Asmolov E S 1999 The inertial lift on a spherical particle in a plane Poiseuille flow at large channel Reynolds number *J. Fluid Mech.* **381** 63–87
[3] Martel J M and Toner M 2012 Inertial focusing dynamics in spiral microchannels *Phys. Fluids* **24** 032001
[4] Ramachandraiah H, Ardabili S, Faridi A M, Gantelius J, Kowalewski J M, Mårtensson G and Russom A 2014 Dean flow-coupled inertial focusing in curved channels *Biomicrofluidics* **8** 034117
[5] Fuerstman M J, Lai A, Thurlow M E, Shevkoplyas S S, Stone H A and Whitesides G M 2007 The pressure drop along rectangular microchannels containing bubbles *Lab Chip* **7** 1479–89
[6] Di Carlo D, Irimia D D, Tompkins R G and Toner M 2007 Continuous inertial focusing, ordering, and separation of particles in microchannels *Proc. Natl Acad. Sci. USA* **104** 18892–7
[7] Andersson M A, Hjort K and Klintberg L 2016 Fracture strength of glass chips for high-pressure microfluidics *J. Micromech. Microeng.* **26** 095009
[8] Tiggelaar R M *et al* 2007 Fabrication, mechanical testing and application of high-pressure glass mi-croreactor chips *Chem. Eng. J.* **131** 163–70